Published in "New Phytologist 217 (1): 245–260, 2018" which should be cited to refer to this work.

WRINKLED1 and ACYL-COA:DIACYLGLYCEROL ACYLTRANSFERASE1 regulate tocochromanol metabolism in Arabidopsis

Sébastien Pellaud[1], Alexandre Bory[1], Valentin Chabert[2], Joëlle Romanens[1], Laurie Chaisse-Leal[1], Anh Vu Doan[1], Lucas Frey[1], Andrea Gust[3], Katharina M. Fromm[2] and Laurent Mène-Saffrané[1]

[1]Department of Biology, University of Fribourg, Chemin du musée 10, CH-1700 Fribourg, Switzerland; [2]Department of Chemistry, University of Fribourg, Chemin du musée, 9, CH-1700, Fribourg, Switzerland; [3]Department of Plant Biochemistry, ZMBP – Center for Plant Molecular Biology, University of Tübingen, Auf der Morgenstelle 32, D-72076, Tübingen, Germany

Author for correspondence:
Laurent Mène-Saffrané
Tel: +41 26 800 8808
Email: laurent.mene-saffrane@unifr.ch

Key words: *diacylglycerol acyltransferase1* (*dgat1*), nutrigenomics, tocomonoenol, tocopherol, vitamin E, *wrinkled1* (*wri1*).

Summary

• Photosynthetic organisms such as plants, algae and some cyanobacteria synthesize tocochromanols, a group of compounds that encompasses tocopherols and tocotrienols and that exhibits vitamin E activity in animals. While most vitamin E biosynthetic genes have been identified in plant genomes, regulatory genes controlling tocopherol accumulation are currently unknown.

• We isolated by forward genetics Arabidopsis enhanced *vitamin* E (*eve*) mutants that overaccumulate the classic tocopherols and plastochromanol-8, and a tocochromanol unknown in this species. We mapped *eve1* and *eve4*, and identified the unknown Arabidopsis tocochromanol by using a combination of analytical tools. In addition, we determined its biosynthetic pathway with a series of tocochromanol biosynthetic mutants and transgenic lines.

• *eve1* and *eve4* are two seed lipid mutants affecting the *WRINKLED1* (*WRI1*) and *ACYL-COA:DIACYLGLYCEROL ACYLTRANSFERASE1* (*DGAT1*) genes, respectively. The unknown tocochromanol is 11′-12′ γ-tocomonoenol, whose biosynthesis is VITAMIN E 1 (VTE1) - and VTE2-dependent and is initiated by the condensation of homogentisate (HGA) and tetrahydrogeranylgeranyl pyrophosphate.

• This study identifies the first two regulatory genes, *WRI1* and *DGAT1*, that control the synthesis of all tocochromanol forms in seeds, and shows the existence of a metabolic trade-off between lipid and tocochromanol metabolisms. Moreover, it shows that Arabidopsis possesses a tocomonoenol biosynthetic pathway that competes with tocopherol synthesis.

Introduction

Tocochromanols encompass a group of compounds with a chromanol ring and a variable prenyl side chain, some of which, such as tocopherols and tocotrienols, exhibit vitamin E activity in animals (DellaPenna & Mène-Saffrané, 2011). Our current understanding of tocochromanol biosynthesis derives from biochemical and genetic studies mostly performed in angiosperms that synthesize four different types of tocochromanols according to the prenyl donor condensed to homogentisate (HGA). Tocopherol and tocotrienol biosyntheses use phytyl pyrophosphate (PPP) and geranylgeranyl pyrophosphate (GGPP) as prenyl donors, respectively (DellaPenna & Mène-Saffrané, 2011). For both types of compound, most biosynthetic genes have been identified in several plant genomes (Mène-Saffrané & Pellaud, 2017). A third type of tocochromanol, plastochromanol-8 (PC-8), which results from the condensation of HGA and solanesyl pyrophosphate, was identified in numerous plant species (Kruk *et al.*, 2014). A fourth tocochromanol type named tocomonoenol has been detected in a few unrelated plant species and a biosynthetic pathway involving the condensation of HGA with tetrahydrogeranylgeranyl pyrophosphate (THGGPP) has been proposed (Kruk *et al.*, 2011). In contrast to tocopherol, tocotrienol and PC-8 biosyntheses, which have been well genetically delineated, no tocomonoenol biosynthetic genes are currently known.

Among the organisms used to study tocochromanol biosynthesis in plants, Arabidopsis is by far the one that provided the most knowledge and resources and in which tocochromanol biosynthesis is the best characterized. Since pioneer works that identified the first tocopherol biosynthetic gene (Shintani & DellaPenna, 1998), 17 tocochromanol biosynthetic genes and many biosynthetic mutants have been described in this organism (reviewed by Mène-Saffrané & Pellaud, 2017). Wild-type Arabidopsis accessions naturally accumulate tocopherols and PC-8. Tocotrienols, which have not been detected in wild-type Arabidopsis accessions analyzed to date, are synthesized in Arabidopsis transgenic lines expressing HGA geranylgeranyl transferase genes from Poaceae or in which HGA availability has been

increased by genetic engineering (Cahoon *et al.*, 2003; Karunanandaa *et al.*, 2005; Zhang *et al.*, 2013).

In contrast to our current knowledge on vitamin E biosynthesis, much less is known about the regulatory gene(s) controlling tocochromanol biosynthesis. Several quantitative trait locus (QTL) and genome-wide association (GWA) studies on tocochromanol synthesis have been performed in several plants (References S1). Although numerous loci controlling tocochromanol synthesis have been identified in plant genomes, the few that have been mapped control tocochromanol composition and not synthesis. Thus, the genes regulating tocochromanol synthesis remain largely unknown. Several metabolic engineering studies showed that overexpression of biosynthetic *VITAMIN E* (*VTE*) genes modestly increased tocochromanol accumulation (Karunanandaa *et al.*, 2005). By contrast, overexpression of upstream biosynthetic genes producing tocochromanol precursors increased tocochromanol metabolism much more efficiently (Karunanandaa *et al.*, 2005; Zhang *et al.*, 2013). In addition, feeding experiments of cell cultures with biosynthetic precursors such as HGA and/or phytol strongly increased tocochromanol accumulation (Furuya *et al.*, 1987; Karunanandaa *et al.*, 2005). Thus, it has been previously concluded that the synthesis and availability of biosynthetic precursors is a major mechanism regulating tocochromanol accumulation. In order to identify the genes regulating the availability of tocochromanol precursors in Arabidopsis, we have isolated new tocochromanol mutants by normal phase (NP)-HPLC-FLD. The *enhanced vitamin e* (*eve*) 1 to 8 mutants overaccumulated the classic tocopherols, PC-8, and a tocochromanol unknown in Arabidopsis. By combining analytical and genetic tools, we identified this compound as 11′-12′ γ-tocomonoenol and genetically delineated its biosynthetic pathway. In addition, we mapped both *eve1* and *eve4* and found that tocochromanol synthesis was strongly increased in these Arabidopsis seed lipid mutants. Our results indicate the existence of a trade-off between the lipid and tocochromanol pathways which are both localized in plastids and utilize common biosynthetic precursors.

Materials and Methods

Biological material and growth conditions

The *Arabidopsis thaliana* (L.) Heynh T-DNA *vte5-3* (SALK_122415), *vte5-4* (WiscDsLoxHs157_06H), *geranylgeranyl reductase-1* (*ggr-1*) (SALK_046606), *ggr-2* (SAIL_856_A06), *wrinkled1-3* (*wri1-3*; SALK_085693), *wri1-4* (SALK_008559), and *acyl-coa:diacylglycerol acyltransferase1-4* (*dgat1-4*; SALK_039456) mutants (Columbia (Col-0) background) were obtained from the Nottingham Arabidopsis Stock Center (Nottingham, UK) and the ABX45/*dgat1-2* mutant (Wassilewskija (Ws) background) was obtained from the Versailles Arabidopsis Stock Center (Versailles, France). The ethyl methanesulfonate (EMS)-mutagenized *vte1-1* and *vte2-1* mutants (Col-0 background) have been previously described (Sattler *et al.*, 2004). The transgenic 35S::*HOMOGENTISATE PHYTYL TRANSFERASE1* (*HPT1*) line is in the Col-0 accession (Collakova & DellaPenna, 2003). Styrian pumpkin seed oil (COOP, Basel, Switzerland; lot #41.351.287), rapeseed oil (SABO, Lugano, Switzerland; #J155), linseed oil (Oleificio, Lugano, Switzerland; #M046), and krill oil (Novakrill, Neptune, Canada; #QC804891/1) were purchased in local stores. Sunflower oil was extracted from the Sanluca variety (Syngenta, Basel, Switzerland). Arabidopsis seeds were surface-sterilized and grown on half-strength Murashige and Skoog (MS) medium supplemented with 1% (w/v) sucrose. For *wri1* mutant alleles, plates were supplemented with 2% (w/v) sucrose and 0.1% (v/v) Tween 40. After seed stratification at 4°C for 3 d in the dark, plates were transferred to a growth chamber illuminated with fluorescent tubes (120 μmol photons $m^{-2}\,s^{-1}$) for 16 h d^{-1} at 22°C during the day and 21°C during the night. Seedlings were transferred to Jiffy-7 (Jiffy Products International AS, Stange, Norway) after 7 d and watered once a week with Wuxal® universal fertilizer (Syngenta Agro AG, Commugny, Switzerland) diluted at 2 ml l^{-1} in water.

Seed weight determination

The weight of Arabidopsis seeds was determined from 200 seeds with an analytical balance (Mettler AE 260 Deltarange, Mettler Toledo, Columbus, OH, USA).

Arabidopsis chemical mutagenesis and seed tocochromanol screening

The Arabidopsis *eve1* and *eve4* mutants identified in this study come from an EMS-mutagenized population of transgenic seeds containing the promAt1g51850:*dao1* construct which was originally produced to screen for plant defenses. Details about the construction of this T-DNA are provided in Supporting Information Methods S1. One gram of the *pAt1g51850:dao1-9.3.3* transgenic seeds were imbibed on wet Whatman 3MM paper for 4 d at 4°C in the dark before being dried for 24 h. Seeds were removed from the filter paper and soaked in 200 ml of water containing 0.3% EMS for 8 h. After washing 15 times with 250 ml of water each time, M1 seeds were sown on soil and M2 seeds were collected. Approximately 1200 M2 plants were grown on soil and M3 seeds were collected and analyzed by NP-HPLC for seed tocochromanols.

Genomic DNA preparation, *eve1* mapping and *eve4* Sanger sequencing

For routine plant genotyping, gDNA was prepared from leaves using the Shorty method (Visscher *et al.*, 2010). For Illumina sequencing, gDNA was extracted from 300 mg of leaves using the peqGOLD Plant DNA Mini Kit (Axon Lab, Baden, Switzerland). Sequencing was performed at the Next-Generation Sequencing Platform of the University of Bern (Switzerland) with the Illumina HiSeq2500 sequencer (Illumina Inc., San Diego, CA, USA) using v3 chemistry (100-bp paired-end reads). Candidate mutations for the *eve1* seed phenotype were identified using the online bioinformatic pipeline SNPTRACK (http://genetics.bwh.harvard.edu/snptrack/). For Sanger sequencing of the *dgat1* mutation, three DNA overlapping fragments covering *DGAT1* were amplified by PCR using the three primer pairs included in

Methods S2. PCR products were purified with the QIAquick® PCR purification kit (Qiagen, Hilden, Germany) and sequenced at Fasteris SA (Plan-les-Ouates, Switzerland).

Mutant genotyping

T-DNA mutants were genotyped by PCR, while *eve1* and *eve4* mutants (EMS-mutagenized) were genotyped with derived cleaved amplified polymorphic sequence markers designed with dCAPS Finder 2.0 (http://helix.wustl.edu/dcaps/dcaps.html). All primer sequences are included in Methods S2. The *eve1* and *eve4* PCR fragments were digested for 16 h at 37°C with Alu*I* and Hinf*I*, respectively. PCRs were performed in a TProfessional BASIC 96 thermocycler (Biometra GmbH, Göttingen, Germany) according to standard laboratory protocols. PCR and restriction products were separated and visualized on 1% and 3% (w/v) agarose gels containing ethidium bromide, respectively.

Tocochromanol extraction

Arabidopsis seed tocochromanols were extracted from 5 or 10 mg of dry mature seeds. Seed samples were ground with a mixer mill (Retsch® MM400, Retsch Technology GmbH, Haan, Germany) set at 30 Hz for 15 min in 1.5-ml Safe-Lock Eppendorf® tubes (Eppendorf, Hamburg, Germany) containing two 3-mm glass beads and 450 µl of extraction buffer (300 µl of MeOH, 150 µl of $CHCl_3$, 1 mg ml^{-1} butylated hydroxytoluene (BHT) and various amount of tocol used as an internal standard). After grinding, tubes were briefly spun down and 300 µl of milliQ water and 150 µl of $CHCl_3$ were added. Tubes were then shaken for 5 min at 28 Hz with the mixer mill. The organic (lower) phase was recovered by centrifugation at 2150 ***g*** (Mikro 20, Hettich-Zentrifugen, Lauenau, Germany) for 5 min and transferred to a second 1.5-ml Safe-Lock tube. Extraction of lipophilic compounds from the original samples was repeated two additional times with 150 µl of $CHCl_3$. Combined organic phases were evaporated (Speed-vac™ Plus SC 110A; Savant Instruments Inc., Farmingdale, NY, USA) and resuspended in *n*-hexane. For samples prepared with 5 and 10 mg of Arabidopsis seeds, residues were resuspended in 40 and 80 µl of *n*-hexane, respectively, from which 20 µl was injected into the HPLC system. Edible oils were directly diluted (1/3) in *n*-hexane and 20 µl was injected into the HPLC system. Sunflower seed tocochromanols were extracted as follows: dehulled seeds were crushed in a 2-ml Safe-Lock Eppendorf® tube containing one 5-mm stainless steel bead, 450 µl of *n*-hexane : ethylacetate (9 : 1, v/v), 100 µl of BHT 0.1% (w/v) in MeOH and 5 µg of tocol (internal standard). Seeds were crushed with a mixer mill set at 20 Hz for 30 min. Samples were centrifuged for 5 min at 6800 ***g*** (Mikro 20) and supernatants were transferred to 7-ml collection glass tubes. Pellets were re-extracted two additional times with 450 µl of *n*-hexane : ethylacetate (9 : 1, v/v; second extraction) and 450 µl of *n*-hexane (third extraction). Pooled supernatants were evaporated under a flux of nitrogen and resuspended in 1 ml of *n*-hexane. Before HPLC analysis, a 100-µl aliquot was transferred to a 1.5-ml Safe-Lock Eppendorf® tube and centrifuged for 5 min at 18 000 ***g*** (Mikro 20). Clear supernatants (*c.* 80 µl) were transferred to autosampler glass vials from which 50 µl was analyzed by NP-HPLC-FLD.

Quantification of tocochromanols by NP-HPLC-FLD

Tocochromanols were quantified by NP-HPLC-FLD with an Agilent Infinity 1260 system (Agilent Technologies, Santa Clara, CA, USA). Samples were separated on a LiChroCART® 250 × 4 mm LiChrospher® 100 Diol 5 µm column (Merck KGaA, Darmstadt, Germany) at 25°C with a flow rate of 1.5 ml min^{-1}. The mobile phase used for isocratic separation (35 min) was composed of *n*-hexane and methyl *tert*-butyl ether (96 : 4, v/v). Tocochromanols were detected with the Agilent 1260 Fluorescence detector using excitation and emission wavelengths of 295 and 330 nm, respectively. Tocochromanols were quantified using calibration curves directly constructed using the instrument software Agilent Chemstation (Agilent Technologies) with known amounts of tocopherol and tocotrienol standards (Matreya LLC, State College, PA, USA). As α-tocomonoenol standard is not commercially available, we quantified it with calibration curves constructed with α-tocopherol which shares the same fluorescent chromanol ring. Similarly, γ-tocomonoenol and PC-8 were quantified with γ-tocopherol calibration curves. Automated quantification used the internal standard tocol (Matreya) to normalize sample-to-sample variations introduced at the extraction step and during sample injection.

Purification of tocomonoenols

Tocomonoenol purification was performed with the NP-HPLC-FLD method described in the previous section. Fractions containing α- or γ-tocomonoenol were collected with a fraction collector connected to the HPLC instrument. For nuclear magnetic resonance (NMR) characterization, γ-tocomonoenol was purified from pumpkin seed oil (210 ml) according to Beldean-Galea *et al.* (2010). After extraction of the unsaponifiable material, γ-tocomonoenol was first purified by NP-HPLC according to the protocol described in the previous section. Fractions containing γ-tocomonoenol were re-chromatographed to eliminate γ-tocopherol traces by reverse-phase (RP) HPLC (Kruk *et al.*, 2011).

Separation of 11′-12′ and 12′-13′ tocomonoenol positional isomers

Separation of 11′-12′ and 12′-13′ tocomonoenol positional isomers was achieved using an RP-HPLC instrument coupled to a fluorescence detector using two C18 analytical columns connected in tandem (LiChrospher® 250 × 4 mm; 100 5 µm C18; BGB Analytik AG (Boeckten, Switzerland); and Discovery® 250 × 4.6 mm; 180 5 µm C18; Supelco Analytical, Sigma-Aldrich, St Louis, MO, USA) according to Yamamoto *et al.* (2001).

NMR analysis of γ-tocomonoenol from pumpkin seed oil

One-dimensional ^{1}H, ^{13}C, Distortionless Enhancement by Polarization Transfer (DEPT) DEPT135 and DEPT90 NMR

spectra of pumpkin γ-tocomonoenol (1 mg in 500 µl of $CDCl_3$) were recorded on a Bruker Avance III 500-MHz NMR spectrometer (Bruker, Billerica, MA, USA), while the two-dimensional $^{1}H,^{13}C$-HSQC NMR spectrum was recorded on a Bruker Avance III 400-MHz NMR spectrometer, at 298 K.

Gas chromatography–mass spectrometry (GC-MS) analysis of purified tocomonoenols and their ozonolysis products

The HPLC-purified fractions containing tocomonoenols were evaporated with nitrogen gas and trimethylsilylated at 65°C for 20 min in 25 µl of pyridine and 25 µl of N,O-bis [trimethylsilyltrifluoroacetamide] containing 1% trimethylchlorosilane (Restek, Lisses, France). After cooling down, solvents were removed with nitrogen gas and residues were resuspended in 6 µl of chloroform, from which 5 µl was analyzed by GC-MS in splitless mode (HP 6890). For acetylation, purified tocomonoenols were incubated at 60°C for 15 min in the presence of 50 µl of pyridine and 50 µl of acetic anhydride (Sigma Aldrich, Buchs, Switzerland). After cooling of samples at room temperature, solvents were removed with nitrogen gas. Residues were resuspended in 100 µl of pentane and mixed with 200 µl of pentane solution saturated with ozone kept at −72°C. The reaction was incubated for 3 min, after which solvents were removed with nitrogen gas. Residues were resuspended in 50 µl of dimethyl sulfide and incubated for 30 min at −72°C. Solvent was eliminated with nitrogen gas and residues were resuspended in 5 µl of $CHCl_3$. TMS tocomonoenols and ozonolysis products were analyzed by GC-MS on a 30 m × 250 µm × 0.25 µm HP-5MS column (Agilent). The injection port and detector temperatures were set to 200 and 260°C, respectively. The oven temperature, originally set at 80°C for 1 min, was increased to 200°C at 20°C min^{-1}, and to 300°C at 5°C min^{-1}. The final oven temperature was held for 5 min.

Triacylglycerol (TAG) purification

Total seed lipids were extracted from 10 mg of seeds as described for tocochromanols, except that lipids were resuspended in 80 µl of *n*-hexane and tocol was omitted. An aliquot (8 µl) was loaded on a 20 × 20 cm thin layer chromatography (TLC) silica gel 60 with a 2.5-cm concentrating zone (Merck). TLC was developed with *n*-hexane/diethyl ether/acetic acid (70/30/1; v/v/v). TAGs were revealed with brief staining with iodine vapors and marked. TAGs were scraped off the TLC and transferred to a glass tube containing 500 µl of 0.01% BHT in MeOH before being transesterified into fatty acid methyl esters.

Fatty acid methyl ester analysis

Fatty acid methyl esters were typically prepared from 50 Arabidopsis seeds. Intact seeds were incubated with 1 ml of 5% H_2SO_4 in MeOH (v/v), 50 µl of 0.1% BHT (w/v) in MeOH and 25 µg of triheptadecanoic acid (Sigma Aldrich, Buchs, Switzerland) used as an internal standard. The reaction was carried out in a 7-ml glass tube closed with a cap equipped with a teflon disposable septum (Septum 12 × 0.25 mm PTFE virginal; VWR International GmbH, Dietikon, Switzerland). The transesterification reaction was performed in a digital dry block heater (VWR International GmbH) set at 85°C for 100 min. Tubes were then cooled down at room temperature, briefly centrifuged, and 1.5 ml of 0.9% NaCl (w/v) and 2 ml of *n*-hexane were added. Samples were thoroughly shaken and centrifuged for 5 min at 240 ***g*** (3K18 centrifuge; Sigma). The organic phase was transferred into a new glass tube and the extraction was repeated twice with 2 ml of *n*-hexane each time. The pooled organic phases were evaporated under a flux of nitrogen and resuspended in 300 µl of heptane from which 2 µl was analysed by GC-FID (7980A GC System; Agilent Technologies) on a 30 m × 250 µm × 0.25 µm DB-23 column (Agilent) with a split ratio of 50 : 1. The oven initial temperature was 100°C held for 2 min, followed by an increase at 25°C min^{-1} to 160°C and then at 8°C min^{-1} to 250°C. The temperature of the injection port and detector was 250°C and 270°C, respectively. Fatty acid methyl esters were quantified with calibration curves constructed with the 37 component FAME mix (Supelco).

Statistical analyses

Statistical analyses were performed with Student's *t*-test using a one-tailed distribution. Asterisks in figures and tables indicate statistically significant differences (**, $P < 0.01$; *, $P < 0.05$) while ns (not significant) indicates $P > 0.05$.

Results

The Arabidopsis *wri1* and *dgat1* mutants overaccumulate tocochromanols

We first cloned the *eve1* mutation by next-generation mapping using an F_2 backcrossed population derived from the Col-0 parental accession fertilized with *eve1* pollen. Tocochromanol analysis in progenies of 206 BC1F2 recombinants showed that 23.8% exhibited the *eve1* phenotype while 76.2% were similar to the Col-0 parent (Fig. 1a). This 3 : 1 Mendelian segregation indicates that the *eve1* phenotype is encoded by a single recessive mutation ($\chi^2 = 0.107$; $P < 0.01$). We sequenced two gDNA samples prepared from Col-0 parental and BC1F2 *eve1* leaves, respectively (Fig. S1). Analysis of Illumina reads with the SNPTRACK bioinformatic pipeline showed that a region of chromosome 3 exhibiting a high degree of homozygosity for EMS-induced mutations carried four candidate mutations (Fig. 1b). We isolated insertion mutants for each candidate and quantified tocochromanols in their progenies. Two independent mutants for the *WRINKLED1* gene (AT3G54320), *wri1-3* and *wri1-4*, displayed the enhanced vitamin E phenotype observed in *eve1* seeds (Table 1a). In addition, both *wri1-3 eve1* and *wri1-4 eve1* hybrid seeds accumulated approximately twice as much tocochromanols as controls, indicating a lack of complementation (Table 1a). Collectively, these data demonstrate that the *eve1* phenotype results from mutations of the *WRI1* gene. The *eve1*

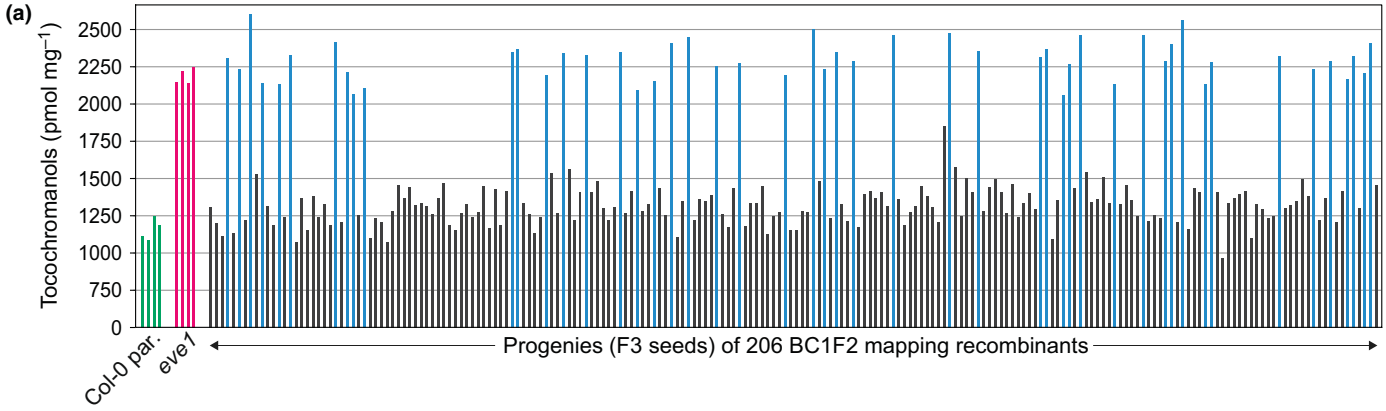

(b)

Chromosome	Position	Mutation	Gene	Consequence /location	Mutant pool coverage (ref./non-ref.)	Par. pool coverage (ref./non-ref.)
3	20 116 058	G-to-A	AT3G54320	Splice site/I5-E6	1/66	80/0
3	20 269 133	G-to-A	AT3G54760	3'-UTR	0/100	61/0
3	20 330 990	G-to-A	AT3G54870	Nonsynonymous/E1	3/67	46/0
3	20 376 410	G-to-A	AT3G54990	Nonsynonymous/E1	1/80	62/0

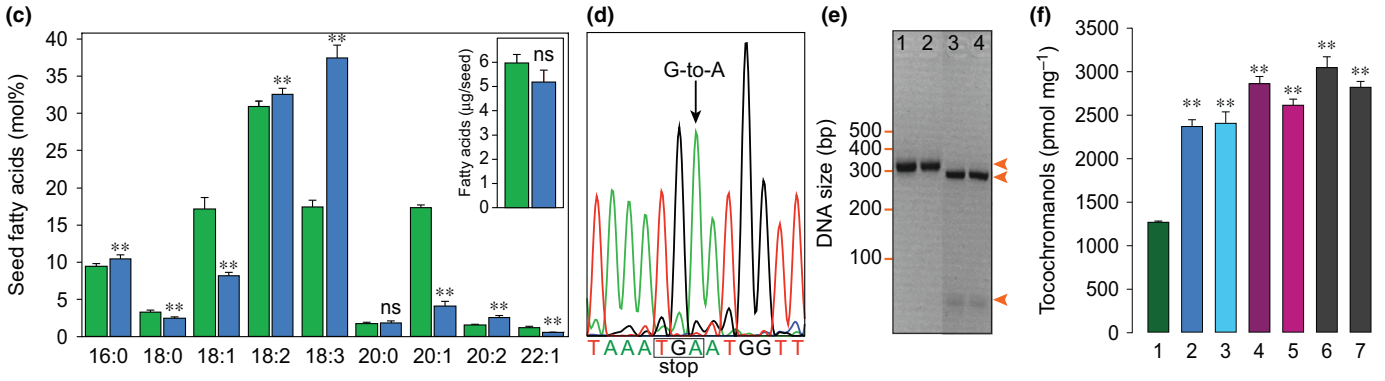

Fig. 1 Identification and mapping of the Arabidopsis *enhanced vitamin e* (*eve*) *1* and *4* mutants. (a) Analysis of seed tocochromanols in progenies of 206 backcross (BC) 1F2 recombinants derived from the pollination of the Columbia (Col-0) parental accession with *eve1* pollen. BC1F3 seeds exhibiting the *eve1* phenotype are colored in blue, while those exhibiting the Col-0 parental phenotype are colored in gray. Four Col-0 parental individuals (green) and *eve1* mutants (purple) were grown together with the BC1F2 mapping population as controls. (b) List of candidate mutations for *eve1* identified by next-generation mapping. Ref. (reference genome) corresponds to the number of aligned reads without the mutation while non-ref. (nonreference genome) corresponds to the number of reads exhibiting the mutation. (c) Seed fatty acid methyl ester composition and amounts in Col-0 parental (green) and the *eve4* mutant (blue). Data are the average ± SD of three independent measurements. (d) DNA electropherogram showing the G-to-A mutation in eve4 At2g19450. (e) *eve4* (*acyl-CoA:diacylglycerol acyltransferase1* (*dgat1-3*))-derived cleaved amplified polymorphism sequence assayed on gDNA prepared from Col-0 parental (1 and 2) and *eve4* (3 and 4) plants. Orange arrows indicate the DNA bands. (f) Seed tocochromanols in Col-0 (1), *wri1-4* (2), *eve1* (*wri1-6*; 3), *eve4* (*dgat1-3*; 4), *dgat1-4* (5), *wri1-4 eve4* (6), and *eve1 dgat1-4* (7). Tocochromanol values are the average ± SD of six independent measurements. Asterisks indicate statistically significant differences using Student's *t*-test: **, $P < 0.01$; *, $P < 0.05$; ns, not significant ($P > 0.05$). bp, base pair; E1, exon 1; I5-E6, intron5-exon6 splice site; par., parental; UTR, untranslated region.

EMS-induced alteration is a G-to-A mutation affecting the splice site at position 20 116 058 of chromosome 3 (Fig. S2). We designated this new allele *wri1-6* and authenticated it in *eve1* gDNA using a derived Cleaved Amplified Polymorphic Sequence (dCAPS) marker (Fig. S2).

WRI1 is a seed-specific transcription factor that regulates lipogenesis, and previously identified *wri1* mutants were found to accumulate less seed oil (Baud *et al.*, 2007). To determine whether other *eve* mutants isolated during the screen exhibited a lipid phenotype as well, we analyzed their seed oil contents. The *eve4* mutant showed a striking fatty acid phenotype typified by a strong decrease of both 18:1 and 20:1 and an increase of 18:3 (Fig. 1c). Searches in the Arabidopsis Lipid Mutant database (http://aralip.plantbiology.msu.edu) revealed that this seed phenotype has been previously observed in mutants of the *ACYL-COA:DIACYLGLYCEROL ACYLTRANSFERASE1* gene, which encodes the last enzyme involved in seed oil synthesis. We amplified $DGAT1_{eve4}$ by PCR, sequenced it, and found a G-to-A mutation converting tryptophan 419 into a premature stop codon (Fig. 1d). As Sanger sequencing of $DGAT1_{eve4}$ was performed on PCR products that may contain errors, we authenticated this mutation in $gDNA_{eve4}$ with a dCAPS marker. While restriction of the *eve4* allele produced two DNA fragments of 285 and 39 bp, respectively, the 324-bp wild-type *DGAT1* allele

Table 1 Seed tocochromanol quantification including γ-tocomonoenol in Arabidopsis *wrinkled1* (*wri1*) and *acyl-coa:diacylglycerol acyltransferase1* (*dgat1*) mutants; seed tocochromanol quantification in (a) *wri1* mutants and (b) *dgat1* mutants

Genotypes	Total tocs	α-toc	γ-toc	γ-t1	PC-8	δ-toc
(a) Seed tocochromanols in Arabidopsis *wri1* mutants						
Col-0 WT	926.0 ± 25.1	14.4 ± 0.4	807.4 ± 22.5	3.5 ± 0.8	78.0 ± 1.2	22.8 ± 1.8
wri1-3	1936.2 ± 135.9**	23.3 ± 5.0**	1712.6 ± 113.9**	31.6 ± 16.4*	116.1 ± 6.6**	52.6 ± 3.9**
wri1-4	1921.0 ± 100.9**	18.8 ± 2.0**	1718.3 ± 87.1**	20.0 ± 1.2**	106.1 ± 6.3**	58.6 ± 5.0**
Col-0 par.	981.5 ± 52.7	11.5 ± 1.2	862.1 ± 46.9	4.5 ± 1.1	80.0 ± 3.4	23.5 ± 1.5
eve1 (*wri1-6*)	1851.5 ± 51.9**	17.3 ± 1.2**	1547.6 ± 37.7**	130.2 ± 19.1**	109.6 ± 2.8**	46.8 ± 3.4**
wri1-3 wri1-6 hybrids	2022.3	32.6	1761.4	55.3	123.9	49.0
wri1-4 wri1-6 hybrids	2113.2	16.1	1893.3	41.7	104.1	58.0
(b) Seed tocochromanols in Arabidopsis *dgat1* mutants						
Col-0 WT	1035.3 ± 97.2	22.1 ± 2.1	894.0 ± 84.3	5.6 ± 1.2	84.1 ± 4.4	30.9 ± 8.4
dgat1-4	2688.0 ± 230.1**	25.2 ± 1.4*	2224.5 ± 227.4**	29.6 ± 9.1**	132.4 ± 13.4**	276.2 ± 15.7**
Col-0 par.	1192.8 ± 65.5	20.5 ± 1.5	1035.5 ± 58.4	9.8 ± 0.8	90.3 ± 5.3	36.7 ± 2.7
eve4 (*dgat1-3*)	2416.6 ± 277.5**	22.7**±2.0	2057.6 ± 247.4**	18.2 ± 2.5**	126.4 ± 7.8**	191.6 ± 28.0**
Ws-0	1010.7 ± 60.0	20.7 ± 1.3	889.2 ± 51.2	2.8 ± 0.7	79.1 ± 3.9	18.9 ± 4.8
ABX45 (*dgat1-2*)	2133.3 ± 30.3**	26.2 ± 1.6**	1867.7 ± 23.4**	13.9 ± 2.2**	109.0 ± 4.1**	116.5 ± 4.4**
dgat1-3 dgat1-4 hybrids	2608.6	42.3	2279.8	14.0	139.2	133.2
DGAT1 dgat1-3 hybrids	1120.2	33.7	988.7	1.9	82.0	15.7
DGAT1 dgat1-4 hybrids	1553.4	33.5	1395.3	8.1	95.7	28.9

Tocochromanol values (pmol mg^{-1}) are the average ± SD of five independent measurements. Asterisks indicate statistically significant differences using Student's *t*-test: **, $P < 0.01$; *, $P < 0.05$; ns, not significant ($P > 0.05$). par., parental; PC-8, plastochromanol-8; t1, tocomonoenol; toc, tocopherol; WT, wild-type.

remained undigested (Fig. 1e). This confirmed that the *eve4* mutant carries a mutated *DGAT1* gene that we designated *dgat1-3*. Analysis of seed tocochromanols in *eve4* and two independent *dgat1* mutants (*dgat1-2* and *dgat1-4* in Ws and Col-0 backgrounds, respectively) showed that *dgat1* seeds accumulated between 2.0 and 2.6 times more tocochromanols than controls (Table 1b). In addition, individual and total tocochromanol contents of *eve4 dgat1-4* hybrid seeds were similar to those of both parents, indicating a lack of complementation (Table 1b). We also quantified tocochromanols in *DGAT1 dgat1-3* and *DGAT1 dgat1-4* seeds. In *DGAT1 dgat1-3* hybrids, tocochromanol contents were similar to that of wild-type controls, suggesting that *dgat1-3* is recessive for seed tocochromanols (Table 1b). By contrast, *DGAT1 dgat1-4* hybrids accumulated 30% more total tocochromanols than controls, indicating that *dgat1-4* is semi--dominant for seed tocochromanols (Table 1b). Collectively, these data demonstrate that *dgat1* mutations induce an enhanced tocochromanol phenotype in Arabidopsis seeds. In addition, they show that two physiologically related genes involved in fatty acid synthesis/oil deposition restrict tocochromanol synthesis in Arabidopsis seeds. Seed tocochromanol contents in two independent *wri1 dgat1* double mutants were comparable to those of the *dgat1* parents (Fig. 1f). The lack of a major additive effect between *wri1* and *dgat1* mutations suggests that the enhancement of tocochromanol metabolism in both mutants might proceed from the same mechanism.

Enhancement of 11′-12′ γ-tocomonoenol synthesis in *eve1* and *eve4* mutants

Detailed analysis of individual tocochromanols in *eve1*(*wri1*) and *eve4*(*dgat1*) seeds showed that they overaccumulated the classic γ-tocopherol (1.8- to 2.5-fold), δ-tocopherol (2.0- to 8.9-fold), PC-8 (1.4- to 1.6-fold), and α-tocopherol (1.2- to 1.6-fold; Table 1a,b). Seeds of *dgat1* mutants exhibited a secondary tocochromanol phenotype as δ-tocopherol contents were much higher than those of any other tocochromanols (up to 8.9 times; Table 1b). In addition, FLD chromatograms of three independent *wri1* and *dgat1* mutants, respectively, exhibited an unknown peak immediately after γ-tocopherol (Figs 2a,b, S3, S4). As chromatograms were recorded with a fluorescence detector that confers a strong chemical specificity, the compound probably carries a chromanol ring that fluoresces at the selected wavelengths. However, its retention time did not match any tocochromanols known to accumulate in wild-type Arabidopsis seeds or tocotrienols that accumulate in some Arabidopsis transgenic lines (Karunanandaa *et al.*, 2005; Zhang *et al.*, 2013). These findings suggest that the Arabidopsis *wri1* and *dgat1* mutants probably overaccumulate a tocochromanol that has not yet been identified in Arabidopsis seeds.

To identify this compound, we purified it, and analyzed it by GC-MS. Searches for *m/z* 223, which corresponds to a fragment of the γ-tocochromanol ring, and later for *m/z* 486 showed a peak in both seed extracts (Fig. 2c,d). The mass spectrum associated with this peak exhibited the ions 73, 223 and 263 also observed in similar proportions in both γ-tocopherol and γ-tocotrienol mass spectra (all trimethylsilyl derivatives; Fig. 2e). These data confirm that the compound found in Arabidopsis has a chromanol ring substituted with two methyl groups. However, while the molecular ions of γ-tocopherol and γ-tocotrienol are equal to 488 and 482, respectively, that of the compound was equal to 486 (Fig. 2e). These data indicate that, in contrast to the fully saturated prenyl side chain of γ-tocopherol and to the tri-unsaturated one of γ-tocotrienol, the prenyl side chain of the

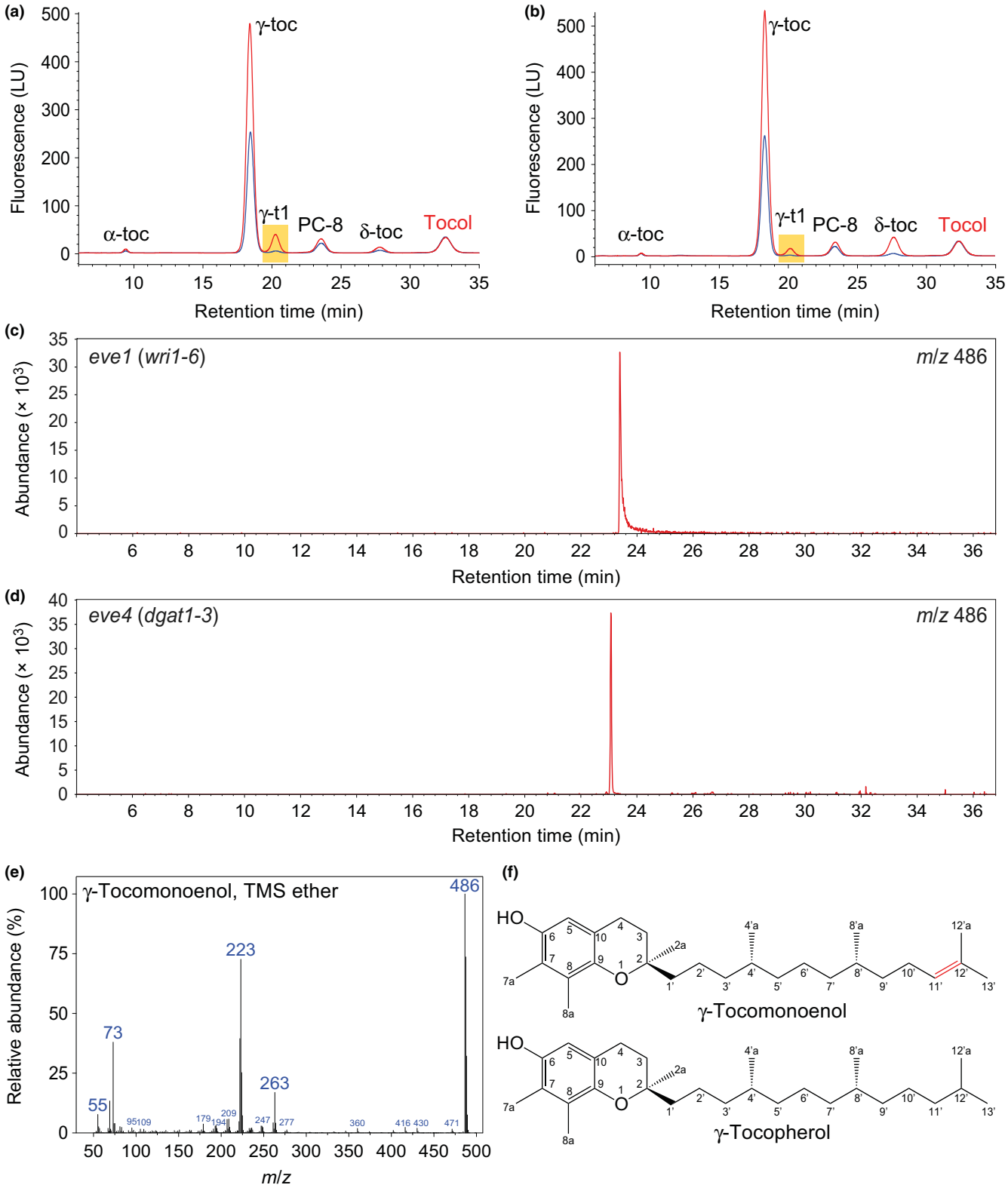

Fig. 2 Accumulation of γ-tocomonoenol in the Arabidopsis *enhanced vitamin e* (*eve*) *1* and *4* seeds. (a, b) Representative seed tocochromanol profiles of (a) the *eve1* (*wrinkled1-6* (*wri1-6*)) mutant (red), (b) the *eve4* (*acyl-CoA:diacylglycerol acyltransferase1-3* (*dgat1-3*)) mutant (red), and (a, b) Columbia (Col-0) wild-type controls (blue). The internal standard, tocol, is labeled in red. (c, d) Gas chromatography–mass spectrometry (GC-MS) analysis (*m/z* 486) of γ-tocomonoenol (TMS ether) purified from *eve1* and *eve4* seeds. (e) Mass spectrum of TMS ether purified from *eve1* seeds. (f) Chemical structures and carbon numbering of 11′-12′ γ-tocomonoenol and γ-tocopherol. LU, light unit; PC-8, plastochromanol-8; t1, tocomonoenol; TMS, trimethylsilyl; toc, tocopherol.

unknown Arabidopsis tocochromanol probably carries a single unsaturation. We searched the literature for this type of tocochromanol and found that few species accumulate tocomonoenols, a group of tocochromanols with a mono-unsaturated prenyl side chain (Matsumoto *et al.*, 1995; Puah *et al.*, 2007; Fiorentino *et al.*, 2009; Butinar *et al.*, 2011; Kruk *et al.*, 2011; Fig. S5). The mass spectrum of the compound found in *eve1* and *eve4* seeds and its chromatographic behavior in NP-HPLC were both identical to those of γ-tocomonoenol identified in pumpkin seeds (Butinar *et al.*, 2011). This suggests that Arabidopsis *eve1* and *eve4* seeds probably accumulate γ-tocomonoenol. Two previous NMR studies on α- and γ-tocomonoenol purified from higher plant material both located the double bond between C-11′ and C-12′ (Matsumoto *et al.*, 1995; Fiorentino *et al.*, 2009). As γ-tocomonoenol is the precursor of α-tocomonoenol, it probably carries its unsaturation at the same location (Fig. 2f). By contrast, α-tocomonoenol produced by phytoplankton exhibits the double bond between C-12′ and C-13′ (Yamamoto *et al.*, 1999, 2001; Fig. S5). To determine the unsaturation position of Arabidopsis γ-tocomonoenol, we first determined the structure of pumpkin γ-tocomonoenol by NMR and used this characterized isomer to elucidate the structure of the Arabidopsis γ-tocomonoenol. NMR analysis of pumpkin γ-tocomonoenol showed that chemical shifts of H and C atoms in position 11′ ($\delta(H^{11'}) = 5.11$ ppm; $\delta(C^{11'}) = 125.1$ ppm), together with the positive signals observed on DEPT spectra, were unequivocally assigned to a methine group (Figs 3a, S6). Similarly, the ^{13}C chemical shift of C-12′ ($\delta(C^{12'}) = 131.0$ ppm), which was not observable on DEPT spectra, was attributed to a quaternary carbon (Figs 3a, S6). Moreover, the chemical shift assignments previously observed for γ-tocopherol were identical to ours, with the exception of positions 10′, 11′, 12′, 13′ and 12′a which were affected by the presence of the unsaturation between C-11′ and C-12′ (Fig. 3a; Baker & Myers, 1991). In addition, ^{13}C chemical shifts of the chromanol substituents ($\delta(C^{7a}) = 11.9$ ppm; $\delta(C^{8a}) = 11.9$ ppm; $\delta(C^{2a}) = 24.1$ ppm) are typical for a γ-tocochromanol (Baker & Myers, 1991; Ohnmacht *et al.*, 2008). Together, these data show that pumpkin seeds synthesize the 11′-12′ γ-tocomonoenol isomer. We then compared its chromatographic behavior to that of Arabidopsis γ-tocomonoenol in an HPLC system that separates 11′-12′ and 12′-13′ tocomonoenol positional isomers (Fig. 3b; Yamamoto *et al.*, 2001). In this system, γ-tocomonoenol purified from *eve1* and *eve4* seeds produced a unique peak at 21.4 min, indicating that each compound probably corresponds to a single isomer (Fig. 3b). In addition, its retention time was identical to that of the 11′-12′ isomer characterized by NMR, indicating that *eve1*, *eve4* and pumpkin γ-tocomonoenols probably carry the unsaturation at the same position (Fig. 3b). We further investigated this by comparing the ozonolysis products of both *eve1* and *eve4* γ-tocomonoenol to those of 11′-12′ γ-tocomonoenol. Indeed, ozone-mediated cleavage of the 11′-12′ or 12′-13′ isomers produced two products whose theoretical molecular masses were equal to 430 and 458, respectively (Figs 3c, S7). GC-MS analysis of the ozonolysis products of 11′-12′ γ-tocomonoenol (pumpkin), *eve1* γ-tocomonoenol, and *eve4* γ-tocomonoenol (all acetylated) showed a strong signal for *m/z* 388 that corresponded to the deacetylated derivative of the 11′-12′ isomer cleaved by ozonolysis (Fig. 3d). The molecular ion of this compound was equal to 430 and its mass spectrum exhibited the typical fragments produced by acetylated γ-tocochromanol rings (151, 152, 191, and 193; Figs 3e, S7). Together, these experiments conclusively demonstrate that pumpkin seeds and the Arabidopsis *eve1* and *eve4* mutants synthesize 2,7,8-trimethyl-2-(4,8,12-trimethyl-11-tridecenyl)-3,4-dihydrochromen-6-ol (11′-12′ γ-tocomonoenol).

γ-tocomonoenol biosynthesis is VTE1 and VTE2 dependent in Arabidopsis

A closer look on FLD chromatograms of Arabidopsis Col-0 seed extracts showed that they exhibit a small peak at the retention time of γ-tocomonoenol (Fig. 4a,b, blue). We purified the compound from Col-0 seeds and analyzed it by GC-MS after trimethylsilylation. The mass spectrum was identical to that found in both *eve1* and *eve4* seeds, and to that previously published for pumpkin γ-tocomonoenol (Fig. S8). This demonstrates that, in addition to tocopherols and PC-8, wild-type Arabidopsis seeds accumulate a third type of tocochromanol, γ-tocomonoenol. Quantification in Col-0 and Landsberg *erecta* (L*er*) seeds showed that γ-tocomonoenol is a minor compound representing 0.9 and 0.3% of the tocochromanol pool, respectively (Fig. 4c).

We analyzed γ-tocomonoenol accumulation in seeds of the *vte1-1* mutant, which lacks all tocochromanols, and in seeds of the *vte2-1* mutant, which lacks tocopherols but accumulates PC-8 (Sattler *et al.*, 2004). To strengthen our conclusions, lipid extracts of both *vte1-1* and *vte2-1* mutants were prepared with twice as many seeds as in controls. While wild-type FLD chromatograms exhibited a peak of γ-tocomonoenol at 20.5 min, those obtained for *vte1-1* and *vte2-1* extracts did not show any detectable signal at this retention time (Fig. 4a,b). These results demonstrate that γ-tocomonoenol synthesis requires both VTE1 and VTE2 activities in Arabidopsis. We also quantified tocochromanols in seeds of transgenic Arabidopsis plants overexpressing the HGA phytyl transferase *HPT1/VTE2* which condenses HGA with prenyl pyrophosphates. Compared with wild-type Col-0 controls, the 35S::*HPT1* seeds accumulated +66% tocochromanols, including +66% γ-tocopherol and +160% δ-tocopherol (Fig. 4d). These results are in line with the original publication showing the effects of *HPT1* overexpression on tocopherol metabolism in Arabidopsis seeds (Collakova & DellaPenna, 2003). In addition, *HPT1* overexpression increased the γ-tocomonoenol level by +770%, confirming the role of VTE2 in γ-tocomonoenol synthesis.

VTE5 and GGR activities restrict γ-tocomonoenol biosynthesis in Arabidopsis seeds

Studies on tocopherol biosynthesis in Arabidopsis have shown that *c.* 75–80% of their prenyl side chain originates from the recycling of phytol released during chlorophyll catabolism. Free phytol is phosphorylated first by the phytol kinase

(a)

Position	^{1}H	^{13}C	DEPT
2	–	75.5	C
3	1.77 m	31.4	CH2
4	2.68 t	22.3	CH2
5	6.38 s	112.1	CH
6	–	146.2	C
7	–	121.6	C
8	–	125.8	C
9	–	145.7	C
10	–	118.3	C
2a	1.25 s	24.1	CH3
7a	2.14 s	11.9	CH3
8a	2.12 s	11.9	CH3
1′	1.55 s	40.0	CH2
2′	1.39 ov	21.0	CH2
3′	1.3/1.1 ov	37.1	CH2
4′	1.39 ov	32.5	CH
5′	1.3/1.1 ov	37.3	CH2
6′	1.30 ov	24.4	CH2
7′	1.3/1.1 ov	37.4	CH2
8′	1.39 ov	32.7	CH
9′	1.3/1.1 ov	37.5	CH2
10′	1.98 m	25.6	CH2
11′	5.11 t	125.1	CH
12′	–	131.0	C
13′	1.69 s	25.7	CH3
4′a	0.87 d	19.6	CH3
8′a	0.87 d	19.6	CH3
12′a	1.61 s	17.6	CH3
OH	4.20 s	–	–

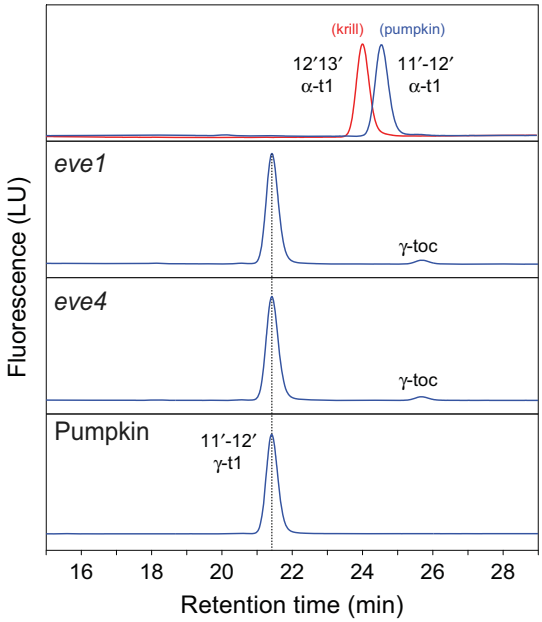

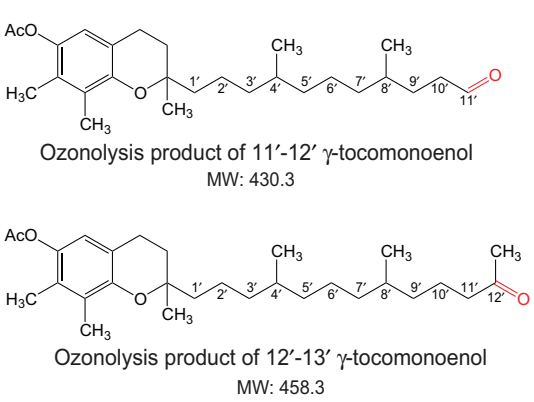

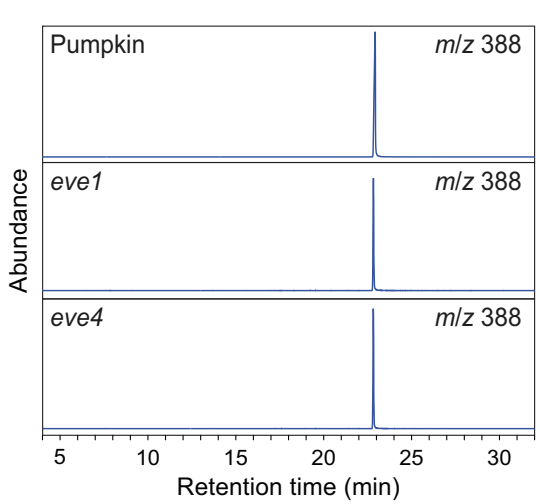

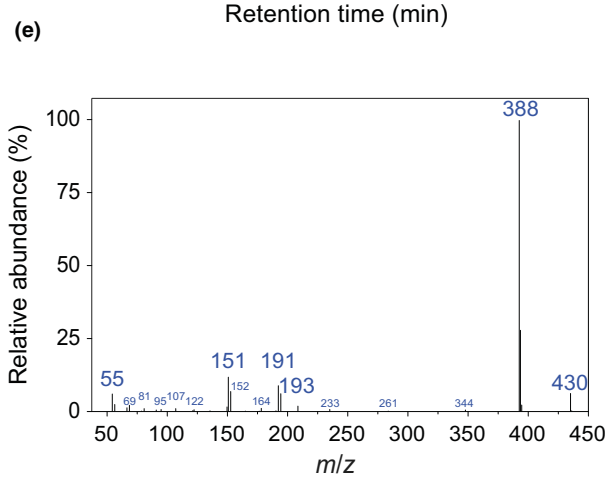

Fig. 3 Structural characterization of Arabidopsis and pumpkin γ-tocomonoenol. (a) ^{1}H, ^{13}C nuclear magnetic resonance (NMR) chemical shifts and distortionless enhancement by polarization transfer signature of γ-tocomonoenol purified from pumpkin seed oil. (b) Chromatographic behaviors of 11′-12′ γ-tocomonoenol (determined by NMR) and *enhanced vitamin e 1* (*eve1*) and *eve4* γ-tocomonoenol in a high-performance liquid chromatography (HPLC) system composed of two C18 columns connected in tandem. The presence of γ-tocopherol in *eve1* and *eve4* chromatograms is attributable to the fact that this compound was purified from Arabidopsis seed lipid extract only by normal phase (NP) HPLC. By contrast, γ-tocomonoenol purified from pumpkin oil was first purified by NP-HPLC followed by reverse-phase HPLC to eliminate γ-tocopherol. To make sure that this system separates 11′-12′ and 12′-13′ tocomonoenol isomers, 11′-12′ and 12′-13′ α-tocomonoenol isomers purified from pumpkin seed oil and krill oil, respectively, were analyzed. (c) Structure of the ozonolysis products of the 11′-12′ and 12′-13′ γ-tocomonoenol isomer, respectively. Ozone-mediated cleavage of the double bond leaves a carbonyl (red) at position C-11′ or C-12′. (d) Gas chromatography–mass spectrometry chromatograms (*m/z* 388) corresponding to the deacetylated derivative of the 11′-12′ γ-tocomonoenol isomer. (e) Mass spectrum of the ozonolysis products of acetylated γ-tocomonoenol purified from *eve1* seeds. d, doublet; LU, light unit; m, multiplet; ov, overlapped; s, singlet; t, triplet; t1, tocomonoenol; toc, tocopherol.

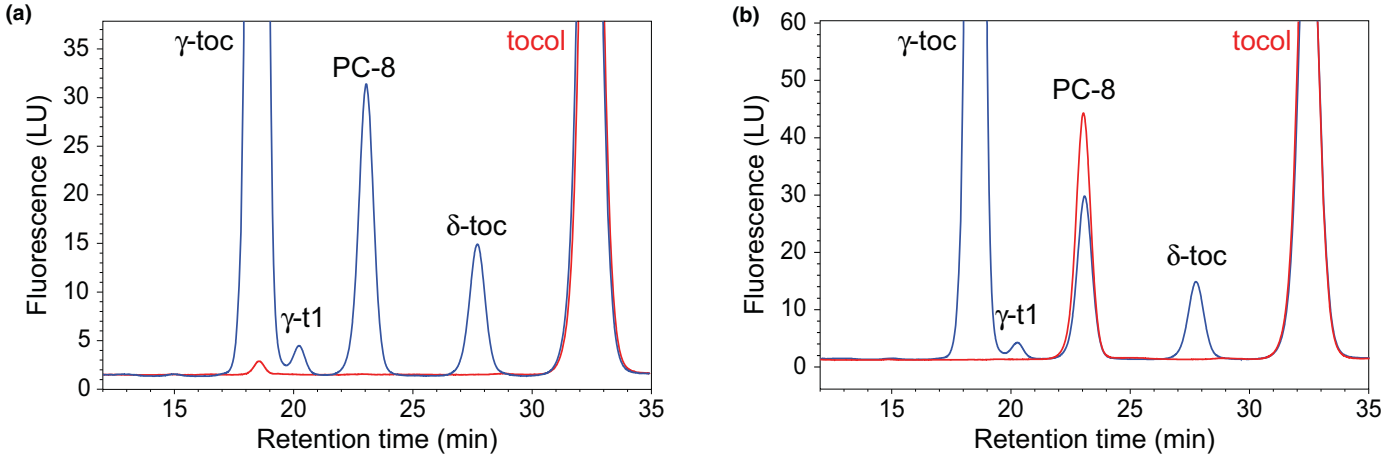

(c)

	Col-0	L*er*	Col-0/L*er*
α-Tocopherol	20.2 ± 2.8	19.0 ± 0.8	1.06^{ns}
γ-Tocopherol	901.0 ± 31.7	854.1 ± 10.3	1.05*
δ-Tocopherol	27.5 ± 2.1	22.0 ± 1.3	1.25**
γ-Tocomonoenol	9.6 ± 1.4	2.7 ± 0.7	3.55**
PC-8	64.0 ± 1.3	46.4 ± 1.9	1.37**
Total tocs	1,022.3 ± 31.5	944.0 ± 9.7	1.08**

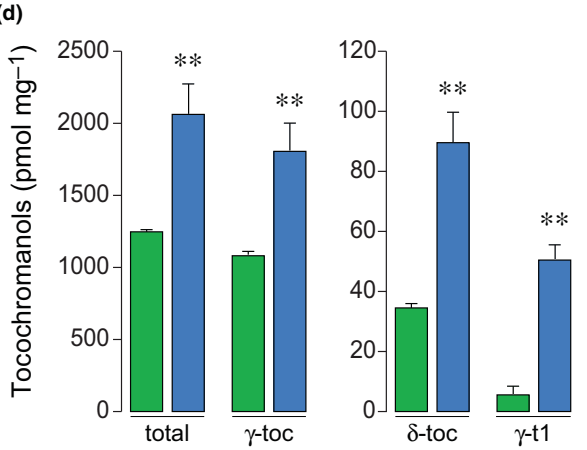

Fig. 4 Biosynthesis of γ-tocomonoenol is VITAMIN E (VTE) 1- and VTE2-dependent. (a, b) Seed tocochromanol profiles of Arabidopsis wild-type controls (blue), (a) the tocochromanol deficient mutant *vte1-1* (red), and (b) the tocopherol-deficient mutant *vte2-1* (red). *vte1-1* and *vte2-1* lipid extracts were prepared with twice as many seeds as for the Columbia (Col-0) wild-type controls. Injection volumes were identical for all genotypes. The internal standard, tocol, is labeled in red. (c) Tocochromanol quantification including γ-tocomonoenol in Col-0 and Landsberg *erecta* (L*er*) seeds. Tocochromanol values (pmol mg^{-1} seed) are the average ± SD of four independent measurements. (d) Quantification of tocochromanols including γ-tocomonoenol in seeds of transgenic Arabidopsis overexpressing the *HOMOGENTISATE PHYTYL TRANSFERASE1 (HPT1, VTE2)* gene (blue) and the Col-0 control (green). Data are the average ± SD of three measurements. α-tocopherol and PC-8 concentrations, which were not significantly different between the two genotypes, are not represented. Asterisks indicate statistically significant differences using Student's *t*-test: **, $P < 0.01$; *, $P < 0.05$; ns, not significant ($P > 0.05$). LU, light unit; PC-8, plastochromanol-8; t1, tocomonoenol; toc, tocopherol.

VTE5 to form phytyl phosphate, which is further phosphorylated by VTE6 to form PPP (Valentin *et al.*, 2006; Vom Dorp *et al.*, 2015). In order to assess the relationship between the tocopherol and tocomonoenol biosynthetic pathways which both require VTE2 activity and HGA, we analyzed seed tocochromanols in two novel Arabidopsis *vte5* T-DNA mutants. The *vte5-3* and *vte5-4* mutations removed 75.5 and 83.6% of tocopherols in Arabidopsis seeds, respectively (Fig. 5a). In contrast to tocopherols, γ-tocomonoenol contents increased 2.3 and 4.0 times in seeds of the *vte5-3* and *vte5-4* mutants, respectively (Fig. 5a). These data show that the tocopherol and tocomonoenol biosynthetic pathways are competing for the VTE2 activity and/or for HGA. This conclusion is further supported by the differences in the degrees of penetrance of the *vte5* mutations, as the lowest tocopherol accumulation induced by the *vte5-4* allele correlated to the highest γ-tocomonoenol accumulation (Fig. 5a). In addition, these data indicate that tocomonoenols probably do not derive from the desaturation of pre-existing tocopherols, as *vte5* mutations decrease tocopherols but increase γ-tocomonoenol.

The current model explaining the origin of the 20–25% of seed tocopherols whose biosynthesis is VTE5-independent relies on the fact that the *GGR* is capable of reducing both geranylgeranylated chlorophyll *a* (Chl*a*) and GGPP to phytylated Chl*a* and PPP, respectively (Keller *et al.*, 1998). Genetic and biochemical studies have shown that geranylgeranyl reductions are sequentially performed, as dihydro- and tetrahydrogeranylgeranyl intermediates were detected when geranylgeranylated chlorophyll was incubated with recombinant GGR, and in Arabidopsis *light-harvesting chlorophyll-binding-like (lil) 3:1* and *lil3:2* single mutants in which GGR activity is reduced (Keller *et al.*, 1998; Tanaka *et al.*, 2010). These data indicate that THGGPP involved in tocomonoenol synthesis might originate from the incomplete desaturation of GGPP. To test this hypothesis, we isolated two hemizygous *GGR ggr* T-DNA mutants (*ggr-1* and *ggr-2*) and

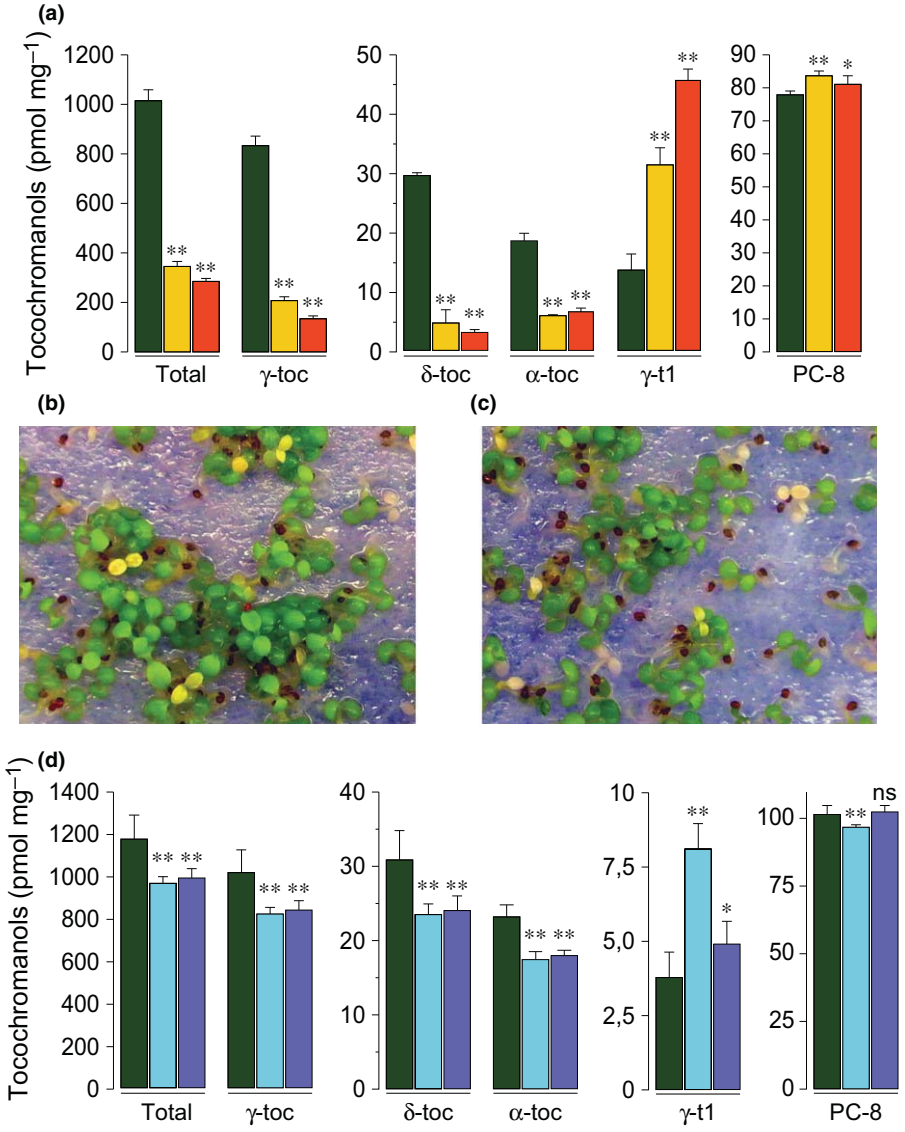

Fig. 5 Seed tocochromanol quantification in Arabidopsis *vitamin e* (*vte*) *5* and *geranylgeranyl reductase* (*ggr*) mutants. (a) Seed tocochromanol content in Columbia (Col-0) (wild-type control; green bars), the *vte5-3* mutant (yellow bars), and the *vte5-4* mutant (orange bars). (b, c) Seedling phenotypes of segregating *GGR ggr* plants. Homozygous (b) *ggr-1* and (c) *ggr-2* individuals are albino. (d) Tocochromanol content in Col-0 (wild-type control; green bars), segregating *GGR ggr-1* (light blue bars), and *GGR ggr-2* seeds (dark blue bars), respectively. Tocochromanol data are the average ± SD of three to five independent seed batches. Asterisks indicate statistically significant differences using Student's *t*-test: **, $P < 0.01$; *, $P < 0.05$; ns, not significant ($P > 0.05$). PC-8, plastochromanol-8; t1, tocomonoenol; toc, tocopherol.

analyzed tocochromanols in their segregating progenies. Indeed, the GGR activity is essential for chlorophyll biosynthesis and homozygous *ggr* mutants are albino and cannot produce seeds (Fig. 5b,c). Mixtures of seeds segregating for *GGR* and *ggr-1* and for *GGR* and *ggr-2* accumulated 19 and 17% less tocopherols compared with wild-type controls, respectively, thus confirming the role of GGR in tocopherol synthesis (Fig. 5d). By contrast, γ-tocomonoenol content significantly increased 2.1- and 1.3-fold in *GGR ggr-1* and *GGR ggr-2* segregating progenies, respectively (Fig. 5d). These data suggest that reduced GGR activity favors tocomonoenol synthesis, probably by limiting the reduction of THGGPP to PPP.

Tocomonoenols are present in common plant oils consumed daily by humans

To date, tocomonoenols have been identified in six plant species and in marine cold-water phytoplankton (Fig. S5). The identification of γ-tocomonoenol in Arabidopsis suggests that oilseed species might also accumulate tocomonoenols. To test this hypothesis, we analyzed whether the oil of several common oilseed crops accumulated or did not accumulate tocomonoenols. In contrast to Arabidopsis seed oil, whose tocochromanol composition is dominated by γ-tocopherol, rapeseed oil quantitatively accumulated both α- and γ-tocopherol forms (Table 2). In addition, rapeseed oil also accumulated small amounts of α- and γ-tocomonoenols (Table 2). Based on these results, we analyzed two other vegetable oils frequently consumed by humans and found that linseed oil accumulated γ-tocomonoenol and sunflower oil accumulated α-tocomonoenol (Table 2). For all three seed oils, the chemical identities of tocomonoenol forms were confirmed by GC-MS (Fig. S9). Collectively, our data demonstrate that tocomonoenols are present in all tested vegetable oils, indicating that their biosynthesis might be conserved in oilseed species.

Table 2 Tocochromanols including tocomonoenol amounts in common plant seed oils

Tocochromanols	Linseed oil	Pumpkin seed oil	Rapeseed oil	Sunflower oil
α-Tocopherol	10.26 ± 0.05	66.58 ± 0.30	505.86 ± 2.74	1072.00 ± 6.35
α-Tocomonoenol	nd	12.65 ± 0.04	3.81 ± 0.17	27.98 ± 0.82
α-Tocotrienol	nd	35.23 ± 0.12	nd	nd
β-Tocopherol	nd	4.93 ± 0.02	5.08 ± 0.07	37.74 ± 0.34
γ-Tocopherol	910.51 ± 5.52	969.16 ± 4.72	685.2.41 ± 2.41	2.00 ± 0.24
γ-Tocomonoenol	1.10 ± 0.01	115.67 ± 0.55	1.23 ± 0.04	nd
γ-Tocotrienol	nd	3.71 ± 0.61	nd	nd
Plastochromanol-8	218.34 ± 1.39	5.30 ± 0.64	74.94 ± 2.05	3.40 ± 0.05
γ-Tocopherol	13.18 ± 0.11	8.88 ± 0.01	17.92 ± 2.04	nd
Total tocochromanols	1153.40 ± 6.89	1222.12 ± 4.53	1294.67 ± 7.50	1139.12 ± 10.71

Tocochromanol quantification in linseed, Styrian pumpkin seed, rapeseed, and sunflower oils, respectively, is shown. Tocochromanol values are expressed in pmol μl^{-1} oil for linseed, pumpkin and rapeseed oils, and in pmol mg^{-1} dehulled seed for sunflower. Measurements are the average ± SD of four independent measurements. The identities of the tocochromanol isoforms colored in red have been confirmed by gas chromatography–mass spectrometry (GC-MS) (Supporting Information Fig. S9). According to the literature, Styrian pumpkin seed oil is the richest source of γ-tocomonoenol known to date (as of August 2017). nd, not detected. Tocomonoenols are shown in red.

Discussion

Previous studies have concluded that the availability of tocochromanol biosynthetic precursors is an important regulatory mechanism controlling vitamin E synthesis in plants (reviewed by Mène-Saffrané & Pellaud, 2017). To date, only the *HOMOGENTISATE DIOXYGENASE* (*HGO1*) gene controlling HGA availability has been shown to alter tocotrienol biosynthesis in soybean (*Glycine max*) (Stacey *et al.*, 2016). By contrast, tocopherol metabolism was not modified in the soybean *hgo1* mutant, and hence tocopherol regulatory genes remained unknown. In order to identify such genes, we isolated Arabidopsis mutants in which tocopherol metabolism is increased. The first identified *eve* mutations affect WRI1 and DGAT1, which are seed-specific proteins involved in fatty acid synthesis and TAG assembly, respectively (Fig. 1; Cernac & Benning, 2004; Zou *et al.*, 1999). In agreement with this, both *eve1* and *eve4* mutants accumulated less fatty acids and TAGs (Fig. S10a,b). Reduced lipid synthesis has been previously associated with a 5–20% decrease of *wri1* seed weight (Baud *et al.*, 2007). As the enhancement of tocochromanol metabolism in *eve* seeds was deduced from tocochromanol data expressed per mg seeds, we determined *wri1* and *dgat1* seed weights. Despite lower lipid contents, *dgat1* seeds were not significantly lighter than controls (Fig. S10c). The *wri1-4* and *eve1* seeds were 21 and 4.5% lighter than controls, respectively (Fig. S10c). Although these data indicate that tocochromanol enhancement is slightly overestimated, notably in *wri1-4*, they are not sufficient to explain the two-fold increase in tocochromanols measured in *wri1* seeds (Table 1). Collectively, these results confirm the genuine enhancement of tocochromanol metabolism in both *wri1* and *dgat1* seeds. Both phytyl and solanesyl branches of the tocochromanol pathway were stimulated in these mutants. Interestingly, in contrast to other tocochromanol mutants or transgenic plants in which tocochromanol metabolism has been enhanced, *wri1* and *dgat1* mutants did not accumulate any tocotrienols (Fig. 3a,b; Karunanandaa *et al.*, 2005; Zhang *et al.*, 2013; Stacey *et al.*, 2016). This suggests that, although HGA content is probably enhanced in *wri1* and *dgat1* to support increased tocochromanol synthesis, the prenyl pyrophosphate metabolism producing the phytyl side chain is very probably enhanced too, thus preventing the synthesis of tocotrienols.

To understand the inverse relationship between WRI1- and DGAT1-mediated lipogenesis and tocochromanol synthesis, we examined their respective biosynthetic pathways. Fatty acid synthesis occurs in plastids and requires the successive conversion of phosphoenolpyruvate (PEP) into pyruvate (PYR), acetyl-CoA and malonyl-CoA (Bates *et al.*, 2013). TAG synthesis occurs in the endoplasmic reticulum and notably involves DGAT1 (Bates *et al.*, 2013). Although DGAT1 is not directly involved in fatty acid synthesis, it was previously shown that *dgat1* mutations lower fatty acid metabolism (Fig. S10a). In addition, it was shown that WRI1 pushes carbon into lipogenesis by stimulating the expression of late glycolysis and lipogenesis genes, respectively, while DGAT1 pulls carbon into lipogenesis by condensing diacylglycerol and acyl-CoAs (Vanhercke *et al.*, 2013). Tocochromanol synthesis occurs in plastids as well and is initiated by the condensation of HGA and various prenyl pyrophosphates (Mène-Saffrané & Pellaud, 2017). HGA derives from the degradation of tyrosine produced by the shikimate pathway which is located in plastids and is initiated by the condensation of PEP and erythrose-4-phosphate (Mène-Saffrané & Pellaud, 2017). Tocochromanol prenyl side chains are mostly produced by the methyl erythritol phosphate (MEP) pathway, which is also located in plastids and is initiated by the condensation of PYR and glyceraldehyde-3-phosphate (Vranová *et al.*, 2013; Zhao *et al.*, 2013). Thus, both tocochromanol, via the shikimate and MEP pathways, and fatty acid syntheses occur in plastids and utilize common biosynthetic precursors, namely PEP and PYR. The interconnection of these pathways suggests that the inverse relationship observed between seed lipid and tocochromanol contents, respectively, might be a consequence of the competition between the pyruvate dehydrogenase complex which channels carbon into fatty acid synthesis and deoxyxylulose 5-phosphate synthase (DXS) which channels it into the MEP pathway. In agreement with this hypothesis, transgenic Arabidopsis

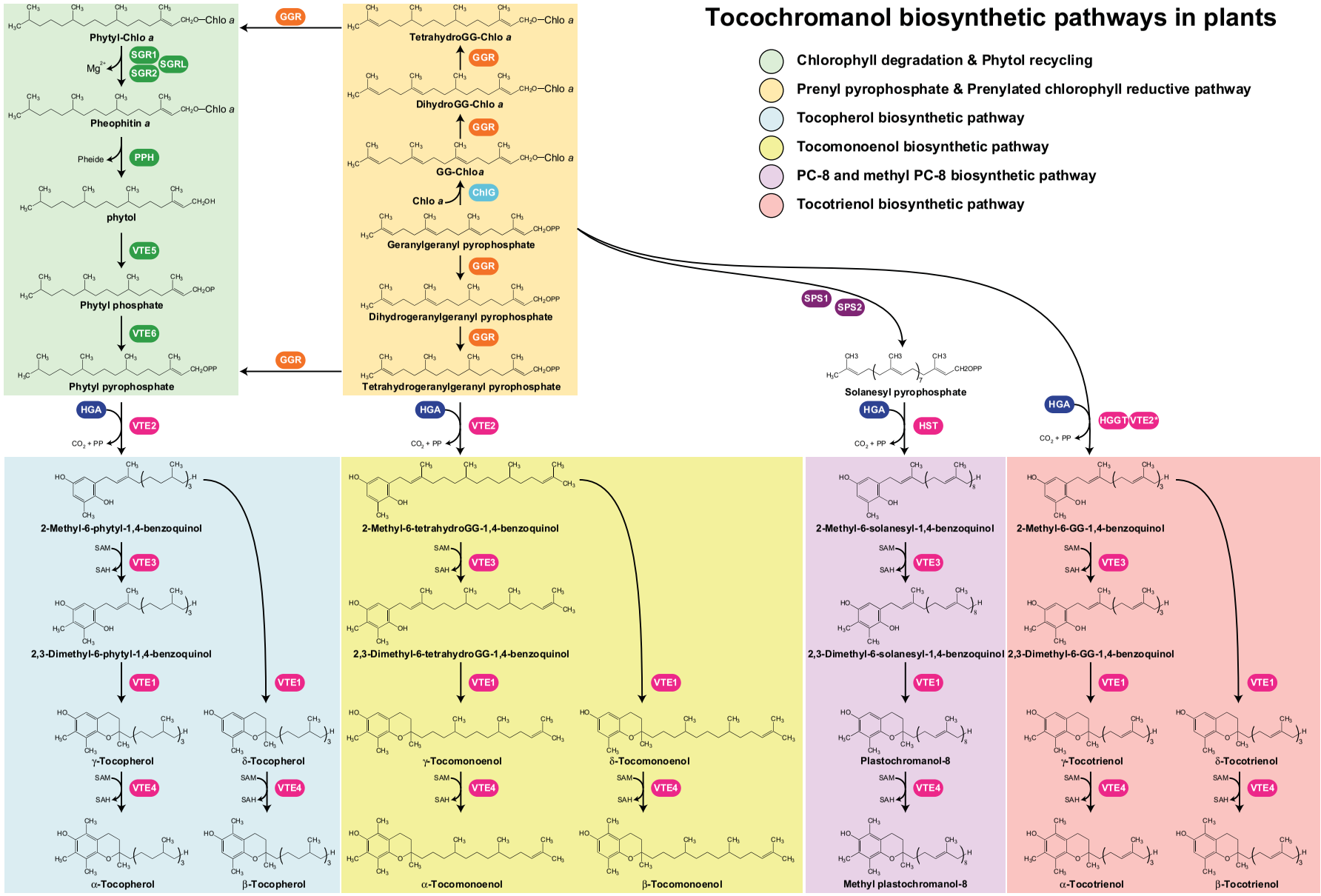

Fig. 6 Tocochromanol biosynthetic pathways in plants. An updated model of the tocochromanol biosynthetic pathways in plants, including the tocomonoenol pathway, is shown. Compounds: Chlo a, chlorophyllide a; GG, geranylgeranyl; HGA, homogentisate; P, phosphate; PP, pyrophosphate; SAH, *S*-adenosyl homocysteine; SAM, *S*-adenosyl methionine. Biosynthetic enzymes: ChlG, chlorophyll synthase; GGR, geranylgeranyl reductase; HGGT, HGA geranylgeranyl transferase; HST, HGA solanesyl transferase; PPH, pheophytinase; SGR and SGRL, stay green and stay green-like (magnesium dechelatases); SPS, solanesyl pyrophosphate synthase; VTE, vitamin E biosynthetic enzyme; VTE1, tocopherol cyclase; VTE2, HGA phytyl transferase; VTE3, methyl transferase; VTE4, γ-tocopherol methyl transferase; VTE5, phytol kinase; VTE6, phytyl phosphate kinase. VTE2* indicates that this prenyl transferase is capable of condensing HGA with GGPP in transgenic plants overaccumulating HGA (Zhang *et al.*, 2013). Methyl PC-8, which has not yet been detected in wild-type plant extracts, has been observed in transgenic Arabidopsis plants overexpressing both the *VTE1* and *VTE4* genes.

plants overexpressing the *DXS* gene were previously shown to accumulate more α-tocopherol in leaves (Estévez *et al.*, 2001). Importantly, only a fraction of the carbon not channeled into fatty acid/TAG synthesis in *wri1* and *dgat1* seeds was converted into tocochromanols (Table 1; Fig. S10a,b). This indicates that a factor(s) other than PYR availability is required to enhance the synthesis of MEP derivatives such as tocochromanols.

A transcriptomic study on developing *wri1* seeds previously showed that this seed-specific Apetala2 transcription factor controls relatively few genes (Ruuska *et al.*, 2002). Interestingly, although tocochromanol metabolism is enhanced in *wri1* seeds, we found that *VTE3* expression (At3g63410) is significantly downregulated in developing *wri1* seeds (Supplementary Table 2 of Ruuska *et al.*, 2002). In addition, other key tocopherol biosynthetic genes present on the custom array including, *VTE1*, *GGR*, *TYROSINE AMINOTRANSFERASE1* (*TAT1,TAT7*), *CHLOROPHYLL SYNTHASE* (*G4,CHLG*) and *GGPPS11*, were not differentially expressed between *wri1* and Col-0 developing seeds (Ruuska *et al.*, 2002; the custom array did not include probes for *VTE2*, *VTE5,* and *VTE6*). These expression data further support the idea that the availability of the vitamin E biosynthetic precursor is a significant mechanism regulating tocochromanol accumulation.

Several QTLs for seed vitamin E (QVE) were previously identified in an Arabidopsis Col-0 (high parent) × L*er* (low parent) population (Gilliland *et al.*, 2006). Interestingly, we found that two overlapping QTLs, namely QVE4 for δ-tocopherol and QVE5 for γ-tocopherol, co-localized with *DGAT1* (Fig. S10d). This, combined with the fact that *dgat1* mutants overaccumulate γ-tocopherol and exhibit a secondary δ-tocopherol phenotype (Table 1b), defines *DGAT1* as a candidate of choice for both QTLs. We looked at the *DGAT1* polymorphism between Col-0 and L*er* and found that, while these accessions carry the same *DGAT1* coding sequences, they are polymorphic for the 5′ untranslated region (5′-UTR) and promoter region of this gene. This suggests that *DGAT1* polymorphism might contribute to the differences in tocochromanol accumulation observed between Col-0 and L*er* (Fig. 4c). We further explored this hypothesis by quantifying seed lipids in Col-0 and L*er* seeds according to three different methods. We found that the accession with higher tocochromanol content, Col-0, accumulated much less lipids than L*er* seeds, notably 25% less TAGs (Fig. S10e). Individual fatty acid analysis showed that the additional oil deposited in L*er* seeds came predominantly from the two monounsaturated fatty acids 18:1 and 20:1 (Fig. S10f). Interestingly, increases in these specific fatty acids have been previously observed in transgenic Arabidopsis lines in which fatty acid synthesis was enhanced by overexpressing *DGAT1* (Vanhercke *et al.*, 2013; Van Erp *et al.*, 2014). Collectively, these data extend to the wild-type germplasm the inverse relationship observed between lipid and tocochromanol metabolisms originally observed in laboratory-derived Arabidopsis mutants. Moreover, they suggest *DGAT1* as a promising candidate for QVE4 and/or QVE5.

In addition to tocopherols and PC-8, both *wri1* and *dgat1* mutants overaccumulated γ-tocomonoenol (Table 1; Figs 2, 3). This type of tocochromanol was previously identified in few plant species and in phytoplankton (Fig. S5). Like other tocomonoenols produced by land plants, Arabidopsis and pumpkin synthesize the 11′-12′ γ-tocomonoenol isomer (Fig. 3). By contrast, the marine-derived α-tocomonoenol produced by phytoplankton carries the unsaturation between C-12′ and C-13′ (Yamamoto *et al.*, 1999). This suggests that tocomonoenol synthesis is probably different between higher plants and phytoplankton, in which either the prenyl donor is different or an extra enzymatic activity changes the position of the unsaturation. In addition, both 11′-12′ and 12′-13′ isomers are found in animals such as in human plasma and in the flesh of whales, cold-water fishes and krill, indicating that animals absorb and transport them throughout the body (Yamamoto *et al.*, 1999, 2001; Dunlap *et al.*, 2002). In Arabidopsis, tocomonoenol synthesis, like tocopherol synthesis, is dependent on VTE1 and VTE2 activities (Figs 4, 5). The increase of γ-tocomonoenol and decrease of tocopherol contents in *vte5* seeds suggest that both pathways are competing for the VTE2 activity and/or for HGA availability. Whereas data for the 35S::*VTE2* overexpressors support the first hypothesis (Fig. 4), it was previously shown that exogenous supply of HGA to dark-grown *Phaseolus coccineus* leaves stimulated γ-tocomonoenol synthesis without affecting γ-tocopherol concentrations (Kruk *et al.*, 2011). This indicates that the polar precursor HGA is also limiting for tocomonoenol synthesis, at least in the absence of light. In addition, the *vte5* data suggest that γ-tocomonoenol probably does not originate from the desaturation of existing tocopherols but from the condensation of HGA with THGGPP, an intermediate in the reductive pathway of GGPP to PPP previously identified in plants (Keller *et al.*, 1998; Tanaka *et al.*, 2010). Data for the *GGR ggr* segregating mutants showing an increase in γ-tocomonoenol accumulation further support this hypothesis. A synoptic model of the plant tocochromanol biosynthetic pathways combining data from previous studies with the data presented here is shown in Fig. 6.

Acknowledgements

We are grateful to Alice Baux from Agroscope (Changins, Switzerland) for providing the sunflower seeds and to Prof. Claude Bron from the Foundation of Research in Biochemistry and on Vitamins (Epalinges, Switzerland) for a financial contribution to the purchase of the analytical instruments. This work was funded by the University of Fribourg, Switzerland. The authors declare no competing financial interests.

Author contributions

S.P. performed experiments and wrote the Methods section. A.B., J.R. performed experiments. V.C. and K.M.F. analyzed the γ-tocomonoenol unsaturation position and wrote the NMR section. L.C-L. analyzed the sunflower oil. L.F. and A.V.D. isolated the *vte5* and *ggr* mutants. A.G. produced the EMS-mutagenized population. L.M-S. conceived the work, performed experiments, and wrote the manuscript. All the authors discussed, commented on and approved the manuscript.

References

Baker JK, Myers CW. 1991. One-dimensional and two-dimensional ^{1}H- and ^{13}C-nuclear magnetic resonance (NMR) analysis of vitamin E raw materials or analytical reference standards. *Pharmaceutical Research* **8**: 763–770.

Bates PD, Stymne S, Ohlrogge J. 2013. Biochemical pathways in seed oil synthesis. *Current Opinion in Plant Biology* **16**: 358–364.

Baud S, Santos Mendoza M, To A, Harscoët E, Lepiniec L. 2007. WRINKLED1 specifies the regulatory action of LEAFY COTYLEDON2 towards fatty acid metabolism during seed maturation in Arabidopsis. *Plant Journal* **50**: 825–838.

Beldean-Galea MS, Horga C, Coman MV. 2010. Separation and determination of tocopherols in vegetable oils by solid phase extraction on porous polymers SPE cartridges and capillary gas chromatography analysis. *Central European Journal of Chemistry* **8**: 1110–1116.

Butinar B, Bucar-Miklavcic M, Mariani C, Raspor P. 2011. New vitamin E isomers (gamma-tocomonoenol and alpha-tocomonoenol) in seeds, roasted seeds and roasted seed oil from the Slovenian pumpkin variety *'Slovenska golica'. Food Chemistry* **128**: 505–512.

Cahoon EB, Hall SE, Ripp KG, Ganzke TS, Hitz WD, Coughlan SJ. 2003. Metabolic redesign of vitamin E biosynthesis in plants for tocotrienol production and increased antioxidant content. *Nature Biotechnology* **21**: 1082–1087.

Cernac A, Benning C. 2004. *WRINKLED1* encodes an AP2/EREB domain protein involved in the control of storage compounds biosynthesis in Arabidopsis. *Plant Journal* **40**: 575–585.

Collakova E, DellaPenna D. 2003. Homogentisate phytyltransferase activity is limiting for tocopherol biosynthesis in Arabidopsis. *Plant Physiology* **131**: 632–642.

DellaPenna D, Mène-Saffrané L. 2011. Vitamin E. *Advances in Botanical Research* **59**: 179–227.

Dunlap WC, Fujisawa A, Yamamoto Y, Moylan TJ, Sidell BD. 2002. Notothenioid fish, krill and phytoplankton from Antarctica contain a vitamin E constituent (α-tocomonoenol) functionally associated with cold-water adaptation. *Comparative Biochemistry and Physiology Part B: Biochemistry and Molecular Biology* **133**: 299–305.

Estévez JM, Cantero A, Reindl A, Reichler S, León P. 2001. 1-Deoxy-D-xylulose-5-phosphate synthase, a limiting enzyme for plastidic isoprenoid biosynthesis in plants. *The Journal of Biological Chemistry* **276**: 22901–22909.

Fiorentino A, Mastellone C, D'Abrosca B, Pacifico S, Scognamiglio M, Cefarelli G, Caputo R, Monaco P. 2009. δ-tocomonoenol: a new vitamin E from kiwi (*Actinidia chinensis*) fruits. *Food Chemistry* **115**: 187–192.

Furuya T, Yoshikawa T, Kimura T, Kaneko H. 1987. Production of tocopherols by cell culture of safflower. *Phytochemistry* **26**: 2741–2747.

Gilliland LU, Magallanes-Lundback M, Hemming C, Supplee A, Koornneef M, Bentsink L, DellaPenna D. 2006. Genetic basis for natural variation in seed vitamin E levels in *Arabidopsis thaliana. Proceedings of the National Academy of Sciences, USA* **103**: 18834–18841.

Karunanandaa B, Qi Q, Hao M, Baszis SR, Jensen PK, Wong YHH, Jiang J, Venkatramesh M, Gruys KJ, Moshiri F *et al.* 2005. Metabolically engineered oilseed crops with enhanced seed tocopherol. *Metabolic Engineering* **7**: 384–400.

Keller Y, Bouvier F, D'Harlingue A, Camara B. 1998. Metabolic compartmentation of plastid prenyllipid biosynthesis. *European Journal of Biochemistry* **251**: 413–417.

Kruk J, Pisarski A, Szymanska R. 2011. Novel vitamin E forms in leaves of *Kalanchoe daigremontiana* and *Phaseolus coccineus. Journal of Plant Physiology* **168**: 2021–2027.

Kruk J, Szymanska R, Cela J, Munne-Bosch S. 2014. Plastochromanol-8: fifty years of research. *Phytochemistry* **108**: 9–16.

Matsumoto A, Takahashi S, Nakano K, Kijima S. 1995. Identification of new vitamin E in plant oil. *Journal of Japan Oil Chemists' Society* **44**: 593–597.

Mène-Saffrané L, Pellaud S. 2017. Vitamin E biofortification of crops. *Current Opinion in Biotechnology* **44**: 189–197.

Ohnmacht S, West R, Simionescu R, Atkinson J. 2008. Assignment of the ^{1}H and ^{13}C NMR of tocotrienols. *Magnetic Resonance in Chemistry* **46**: 287–294.

Puah CW, Choo YM, Ma AN, Chuah CH. 2007. The effect of physical refining on palm vitamin E (tocopherol, tocotrienol and tocomonoenol). *American Journal of Applied Sciences* **4**: 374–377.

Ruuska SA, Girke T, Benning C, Ohlrogge JB. 2002. Contrapuntal networks of gene expression during Arabidopsis seed filling. *Plant Cell* **14**: 1191–1206.

Sattler SE, Gilliland LU, Magallanes-Lundback M, Pollard M, DellaPenna D. 2004. Vitamin E is essential for seed longevity and for preventing lipid peroxidation during germination. *Plant Cell* **16**: 1419–1432.

Shintani D, DellaPenna D. 1998. Elevating the vitamin E content of plants through metabolic engineering. *Science* **282**: 2098–2100.

Stacey MG, Cahoon RE, Nguyen HT, Cui Y, Sato S, Nguyen CT, Phoka N, Clark KM, Liang Y, Forrester J *et al.* 2016. Identification of homogentisate dioxygenase as a target for vitamin E biofortification in oilseeds. *Plant Physiology* **172**: 1506–1518.

Tanaka R, Rothbar M, Oka S, Takabayashi A, Takahashi K, Shibata M, Myouga F, Motohashi R, Shinozaki K, Grimm B *et al.* 2010. LIL3, a light-harvesting-like protein, plays an essential role in chlorophyll and tocopherol biosynthesis. *Proceedings of the National Academy of Sciences, USA* **107**: 16721–16725.

Valentin HE, Lincoln K, Moshiri F, Jensen PK, Qi Q, Venkatesh TV, Karunanandaa B, Baszis SR, Norris SR, Savidge B *et al.* 2006. The *Arabidopsis vitamin E pathway gene5-1* mutant reveals a critical role for phytol kinase in seed tocopherol biosynthesis. *Plant Cell* **18**: 212–224.

Van Erp H, Kelly AA, Menard G, Eastmond PJ. 2014. Multigene engineering of triacylglycerol metabolism boosts seed oil content in Arabidopsis. *Plant Physiology* **165**: 30–36.

Vanhercke T, El Tahchy A, Shrestha P, Zhou XR, Singh SP, Petrie JR. 2013. Synergistic effect of WRI1 and DGAT1 coexpression on tricylglycerol biosynthesis in plants. *FEBS Letters* **587**: 364–369.

Visscher AM, Paul AL, Kirst M, Guy CL, Schuerger C, Ferl RJ. 2010. Growth performance and root transcriptome remodeling of Arabidopsis in response to Mars-like levels of magnesium sulfate. *PLoS ONE* **5**: e12348.

Vom Dorp K, Hölzl G, Plohmann C, Eisenhut M, Abraham M, Weber APM, Hanson AD, Dörmann P. 2015. Remobilization of phytol from chlorophyll degradation is essential for tocopherol synthesis and growth of Arabidopsis. *The Plant Cell* **27**: 2846–2859.

Vranová E, Coman D, Gruissem W. 2013. Network analysis of the MVA and MEP pathways for isoprenoid synthesis. *Annual Review of Plant Biology* **64**: 665–700.

Yamamoto Y, Fujisawa A, Hara A, Dunlap WC. 2001. An unusual vitamin E constituent (α-tocomonoenol) provides enhanced antioxidant protection in marine organisms adapted to cold-water environments. *Proceedings of the National Academy of Sciences, USA* **98**: 13144–14148.

Yamamoto Y, Maita N, Fujisawa A, Takashima J, Ishii Y, Dunlap WC. 1999. A new vitamin E (α-tocomonoenol) from eggs of the Pacific salmon *Oncorhynchus keta. Journal of Natural Products* **62**: 1685–1687.

Zhang C, Cahoon RE, Hunter SC, Chen M, Han J, Cahoon EB. 2013. Genetic and biochemical basis for alternative routes of tocotrienol biosynthesis for enhanced vitamin E antioxidant production. *Plant Journal* **73**: 628–639.

Zhao L, Chang WC, Xiao Y, Liu HW, Liu P. 2013. Methylerythritol phosphate pathway of isoprenoid biosynthesis. *Annual Review of Biochemistry* **82**: 497–530.

Zou J, Wei Y, Jako C, Kumar A, Selvaraj G, Taylor DC. 1999. The *Arabidopsis thaliana TAG1* mutant has a mutation in a diacylglycerol acyltransferase gene. *The Plant Journal* **19**: 645–653.

Supporting Information

Additional Supporting Information may be found online in the Supporting Information tab for this article:

Fig. S1 Next-generation mapping of the *enhanced vitamin e 1* mutation.

Fig. S2 Molecular characterization of the *eve1* (*wri1-6*) mutation.

Fig. S3 Seed tocochromanol profiles of independent *wri1* mutants.

Fig. S4 Seed tocochromanol profiles of independent *dgat1* mutants.

Fig. S5 List of organisms producing tocomonoenols.

Fig. S6 NMR spectra of pumpkin 11′-12′ γ-tocomonoenol.

Fig. S7 Determination of the unsaturation position in γ-tocomonoenol.

Fig. S8 Mass spectrum of Col-0 γ-tocomonoenol.

Fig. S9 Mass spectra of tocomonoenols purified from common seed oils.

Fig. S10 *eve1* and *eve4* supplementary data (lipids and QTLs).

Methods S1 Arabidopsis transgenic promAt1g51850:*dao1* line.

Methods S2 List of genotyping and sequencing primers.

References S1 References about tocopherol QTL and GWA studies.

Please note: Wiley Blackwell are not responsible for the content or functionality of any Supporting Information supplied by the authors. Any queries (other than missing material) should be directed to the *New Phytologist* Central Office.